ISSN 1392–1207. MECHANIKA. 2022 Volume 28(3): 242–246

Computational Evaluation of the Effect of Plunger Spring Stiffness on Opening and Closing Times of the Low-Pressure Gas-Phase Injector

Dariusz SZPICA*, Michał KUSZNIER**
**Bialystok University of Technology, Faculty of Mechanical Engineering, 45C Wiejska Str., 15-181 Bialystok, Poland, E-mail: d.szpica@pb.edu.pl*
***Bialystok University of Technology, Doctoral School, 45A Wiejska Str., 15-351 Bialystok; Poland, E-mail: m.kusznier@doktoranci.pb.edu.pl*

crossref http://dx.doi.org/10.5755/j02.mech.31230

1. Introduction

Due to the continuous tightening of clean exhaust standards [1] and the need to meet global emission standards [2], the use of alternative fuels in transportation is being sought. The largest contributor in this area is liquefied petroleum gas (LPG) [3]. For the most part, the use of LPG in internal combustion engine power systems is done as vapor [4, 5], although modern automotive power units require the use of LPG in the liquid phase and with direct injection [6]. Outside of transportation, alternative fuels are used in work machinery [7].

The popularity of alternative LPG vapor power systems is causing an increase in interest in computational methods for evaluating functional parameters. The calculations support the design and manufacturing process as well as are able to evaluate the influence of selected input features of a virtual product on its output parameters. In the case of gas injectors, the output (functional) parameters are mainly opening and closing times and maximum mass flow rate [5, 8, 9].

Modeling the operation of the low-pressure gas-phase injector involving on the combination of mechanical, electrical and hydraulic issues. For the mechanical part, an analytical approach [10, 11] or finite element method (FEM) can be used, which is also successfully used in modeling electromagnetic circuits [12]. Analytical models of electromagnetic circuits [13–15] give high agreement with FEM calculations and experimental studies. For hydraulic calculations to estimate fuel flow rates, analytical models [16, 17], or computational fluid dynamics method (CFD) [18, 19] can be used.

Analyzing the results of calculations included in the literature reports, it was observed that the mathematical models presented there show the existence of time delays of plunger displacement in relation to the forcing resulting mainly from the inertia forces and resistance to motion. Therefore, an attempt has been made to computationally demonstrate the effect of the plunger pressure stiffness on the opening and closing times of the low-pressure gas-phase injector as a way to fill the research gap in this subject. Section 2 of the paper presents the object of analysis, Section 3 the mathematical model adopted in the course of the analysis. In Section 4 the conditions necessary to initiate the calculations are described. The results described in Section 5 were aimed to determine the times of opening and closing of the gas injector with variable stiffness of the plunger pressure spring and the accompanying changes in the time-cross section. Section 6 is a summary of the work in which conclusions are presented. The obtained results can be useful in modeling the operation of an internal combustion engine or in the operational assessment of the gas injector condition.

2. The analysis object

The object of analysis was the Valtek Rail STD Type 30 injector. This injector belongs to the low-pressure gas-phase group. In the unpowered state it is normally closed. When an electrical impulse is applied to the coil terminals, an electromagnetic field is created that lifts the plunger, which is initially pressed against the seat by a spring. After the electric impulse disappears, the injector is closed by the force of the compression spring. A detailed description of the operation will be presented later in this paper. The basic technical data of the analyzed injector have been presented in Table 1.

Table 1

The technical data of the Valtek Rail STD Type 30 [20]

Parameter	Value
Coil resistance	$R = 3\ \Omega$
Plunger displacement	$x_{max} = 0.4\times10^{-3}$ m
Nozzle size	$d = (1.5\ldots3.5)\times10^{-3}$ m
Time to full opening	$t_{tfo} = 3.4\times10^{-3}$ s
Time to closing	$t_{tfc} = 2.2\times10^{-3}$ s
Max. working pressure	$p_{max} = 4.5\times10^{5}$ Pa

3. Modelling of injector operations

The model description is based on the scheme presented in Fig. 1 with the following main simplifying assumptions:

- the movement of the plunger is a result of instantaneous values of the acting forces;
- the thrust force from the air pressure depends on the position of the plunger;
- friction is divided into static, kinetic and viscous, and its value depends on the plunger movement;
- vibrations, mechanical disturbances, eddy currents, magnetic saturation, coil temperature change, plunger aerodynamic drag are omitted.

Based on the descriptions presented in [5, 14, 15, 21, 22] the equilibrium equation of the forces acting on the plunger can be taken as Eq. (1):

$$F_e - F_f - F_s - F_p - F_m = 0. \quad (1)$$

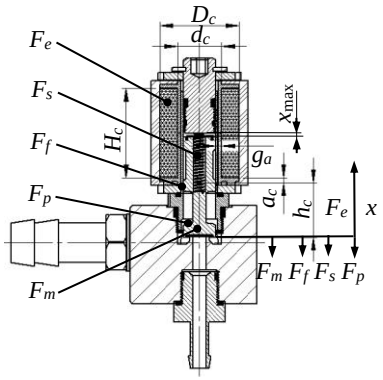

Fig. 1 Diagram presenting main dimensions of the injector and acting forces (description in text)

The waveform of the electromagnetic force F_e resulted from the electromagnetic circuit's characteristic $L(x)$ and the value of the electric current I according to Eq. (2):

$$F_e = \frac{1}{2} I^2 \frac{dL(x)}{dx}. \tag{2}$$

The variation of current I feeding the circuit was calculated based on Eq. (3):

$$\frac{dI}{dt} = \frac{1}{L(x)}\left(U - RI - \frac{dL(x)}{dx}\frac{dx}{dt} I\right). \tag{3}$$

The values of inductance $L(x)$ of the circuit assuming plunger displacement x are written in the form Eq. (4):

$$\frac{dL(x)}{dx} = \frac{\mu_0 \pi a_c^2 \left(\frac{D_c + d_c}{2}\right) N^2}{g_a \left(x + a_c\right)^2}. \tag{4}$$

The friction force was dependent on the position of the plunger (Eq. (5)):

$$F_f = \begin{cases} \mu_s mg \quad \text{if} \quad x = 0, \; x = x_{\max} \\ \left(\mu_k F_N + \mu_v \frac{dx}{dt}\right) sgn(x) \quad \text{if} \quad x \neq 0 \end{cases}. \tag{5}$$

The force from the plunger compression spring was calculated from Eq. (6):

$$F_s = C\left(x_0 + x\right). \tag{6}$$

The force from gas pressure depended on the position of the plunger (Eq. (7)):

$$F_g = \begin{cases} A_1 p_1 + A_2 p_2 \quad \text{if} \quad x = 0 \\ 0 \quad \text{if} \quad x > 1\times10^{-7}\,\text{m} \end{cases}. \tag{7}$$

The inertia force depended on the mass and acceleration of the plunger (Eq. (8)):

$$F_m = m\frac{d^2x}{dt^2}. \tag{8}$$

Finally, the system of equations necessary to determine the current waveform I and the plunger displacement x will take the form Eq. (9):

$$\begin{cases} \frac{dx}{dt} = v \\ \frac{dv}{dt} = \frac{F_e - F_d - F_s - F_p}{m} \\ \frac{dI}{dt} = \frac{1}{L(x)}\left(U - RI - \frac{dL(x)}{dx}\frac{dx}{dt} I\right) \end{cases}. \tag{9}$$

where the designations are as shown in Fig. 1 and Table 2.

4. Parameter values and initial conditions

Table 2 shows the parameter values and boundary conditions necessary to initialize the calculations.

Table 2

Parameter values and initial conditions necessary to initiate the calculation

Parameter	Value
Injection time	$t_{inj} = 5\times10^{-3}$ s
Mass of the piston and needle	$m = 5\times10^{-3}$ kg
Coil dimensions and position	$a_c = 3\times10^{-3}$ m $h_c = 13.86\times10^{-3}$ m $H_c = 23\times10^{-3}$ m $D_c = 20\times10^{-3}$ m $d_c = 11\times10^{-3}$ m $g_a = 1.4\times10^{-3}$ m;
Number of coil windings	$N_c = 500$
Permeability of vacuum	$\mu_0 = 4\times10^{-7}$ H/m
Spring stiffness	$C = 780$ N/m
Initial tension the spring	$x_0 = 0.75\times10^{-3}$ m
Coefficient of static friction	$\mu_s = 0.61$
Coefficient of kinematic friction	$\mu_k = 0.47$
Coefficient of viscous friction	$\mu_v = 0.009$ (Ns)/m
Cross area over the valve	$A_1 = 32.56\times10^{-6}$ m^2
Cross area under the valve	$A_2 = 12.56\times10^{-6}$ m^2
Gas pressure	$p_1 = 1\times10^5$ Pa + p_2
Inlet manifold pressure	$p_2 = 1\times10^5$ Pa
Density of air	$\rho = 1.2$ kg/m^3
Initial conditions ($t = 0$ s)	
Electric voltage	$U = 12$ V
Electric current	$I = 0$ A
Plunger displacement	$x = 0$ m

5. Results and discussion

In each analyzed case, the system of differential Eq. (9) was solved numerically in Matlab/Simulink [23]. The implicit trapezoidal method combined with backward differentiation was used. The integration step was varied, with the mini-minimum value set at 1×10^{-7} s). Matlab/Simulink software allows easy implementation of empirical models, as confirmed in [5, 24, 25].

In the initial part of the analysis, assuming the data and boundary conditions based on Table 2, the od-response

of the system to a pulsed electric voltage forcing U = 12 V with duration t_{inj} = 5×10^{-3} s, with spring stiffness C = =780 N/m was obtained.

The impulse in the form of electric voltage U (from-segment A-D with length t_{inj} = 2.21×10^{-3} s) is an excitation (Fig. 2). In response, the electric current waveform I has characteristic breakthroughs (points B` and $C$`) at the points of beginning of travel (point B) and reaching by the plunger the maximum opening x_{max} (point C). The breakthrough separates the coil inductance values at constant (segments A-B and C-D) and variable plunger position (segment B-C).

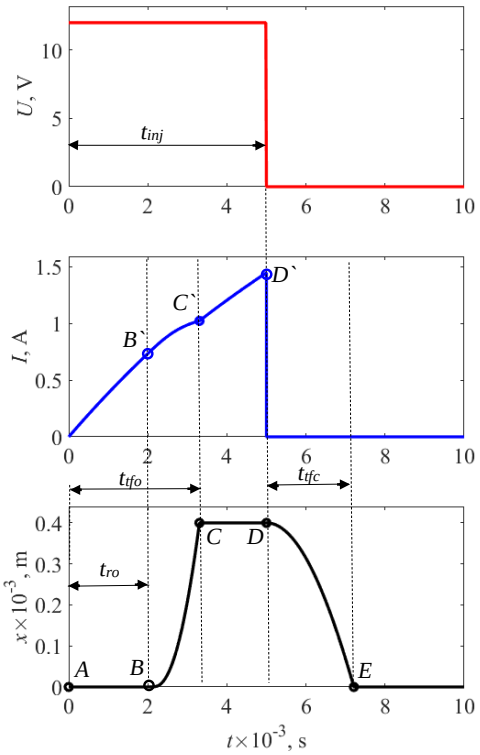

Fig. 2 The runs of input U and response I and x obtained for the purposes of the initial analysis

When an electrical pulse appears at the injector coil terminals, the plunger responds with a delay t_{ro} (Fig. 2). This is due to the need to overcome spring preload, inertia resistance and plunger friction. When the coil supply is lost (points D and D`), the plunger is moved by the force from the compression spring. In this case, the closing delay is not visible, hence the response time cannot be determined.

The plunger lift x enabled determination of the time to full opening (t_{tfo} =3.30×10^{-3} s – point C in Fig. 1) and closing (t_{tfc} = 2.21×10^{-3} s – point D). Comparing the results with the manufacturer's data (Table 1), there was a 2.77% longer time to full opening and 0.50 % shorter time to full closing. Based on this, the proposed injector performance model was found to be representative for comparison purposes.

In the main part of the analysis, the times to full opening and closing of the injector were determined with changes of the stiffness of the compression spring in the range (100...2000) N/m with a step of 100 N/m. The results of the calculations for the times to full opening t_{tfo} and closing t_{tfc} are shown in Table 3.

Table 3

Determined times to full opening and closing of the injector depending on the stiffness spring

t, ×10^{-3} s	C, N/m						
	100	200	300	400	500	600	700
t_{tfo}	3.09	3.12	3.15	3.19	3.22	3.25	3.28
t_{tfc}	6.90	4.57	3.65	3.13	2.78	2.53	2.34
t, ×10^{-3} s	C, N/m						
	800	900	1000	1100	1200	1300	1400
t_{tfo}	3.31	3.34	3.37	3.40	3.43	3.46	3.49
t_{tfc}	2.18	2.05	1.95	1.85	1.77	1.70	1.64
t, ×10^{-3} s	C, N/m						
	1500	1600	1700	1800	1900	2000	
t_{tfo}	3.52	3.55	3.58	3.61	3.64	3.67	
t_{tfc}	1.58	1.53	1.49	1.44	1.40	1.37	

In order to graphically represent the results of the calculations, Fig. 3 was created. The obtained values for the time to full opening t_{tfo} were approximated by a linear function, obtaining high agreement (R^2 = 0.9995). In the case of closing times, a power approximation function was used, where a high agreement was also observed (R^2 = 0.9992). Analyzing the differences in the t_{tfo} times, little change is apparent in the spring stiffness range assumed in the calculations. This means that the electromagnetic field generated by the coil is sufficient even at a stiffness of C = 2000 N/m. Considering the time t_{tfo} as a whole, its 18.85% elongation at 2000 N/m relative to the stiffness of 100 N/m was noted. In the case of time t_{tfc} in the considered spring stiffness range, the time was reduced by 80.17% at 100 N/m relative to 2000 N/m.

The plunger compression spring stiffness loss or gain can occur in the course of operation. On the one hand, wear and tear can cause a decrease in stiffness, while on the other hand, contaminants between the spring coils can cause an increase in stiffness.

Variation in the times t_{tfo} and t_{tfc} can fundamentally affect the functional capability of the injector. In Fig. 4, selected plunger lift waveforms are shown to illustrate the differences in the area fields underneath them. The surface area indirectly illustrates the injector output.

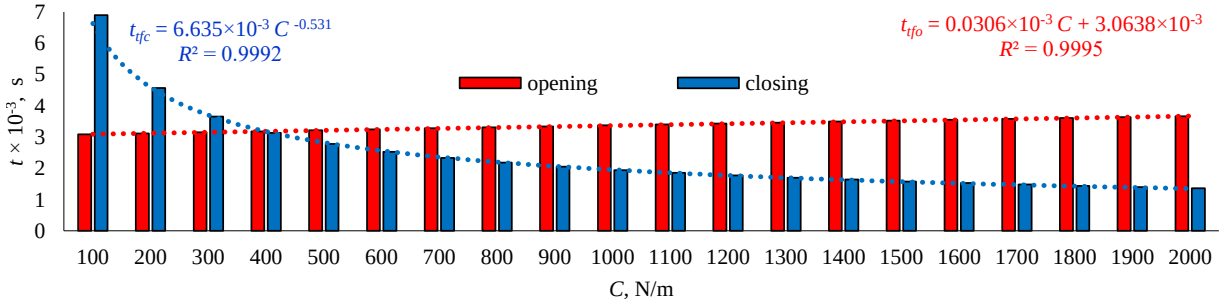

Fig. 3 Determined times to full opening and closing of the injector depending on the stiffness spring

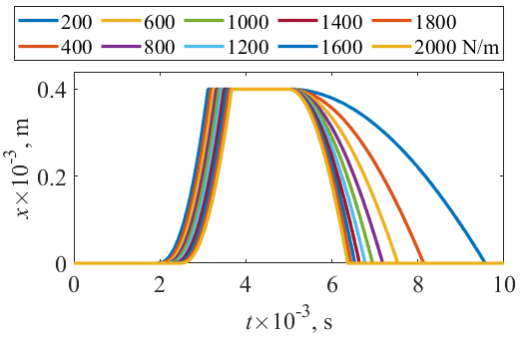

Fig. 4 Selected waveforms of the plunger lift depending on the stiffness of the pressure spring

Therefore, in the final stage of the analysis, the displacement results were interpolated using the linear method to the 1×10^{-7} s step and further determined by integrating the time-cross section of the injector opening using the rectangle method. Fig. 5 shows the determined time-cross section values with 100% representing the highest value obtained with a stiffness of 100 N/m.

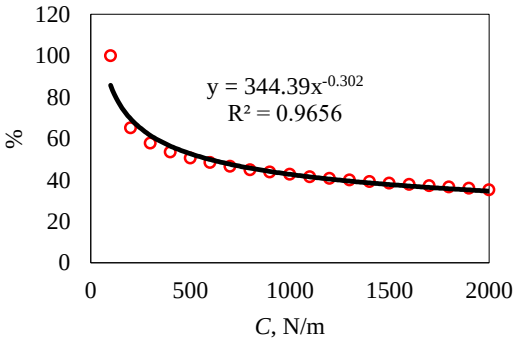

Fig. 5 The time-cross section of the injector

The time-cross section determined at a stiffness of 2000 N/m is only 35.21% of the time-cross section at 100 N/m. From approx. 500 N/m, the time-cross sections decrease linearly with a slight decrease as the stiffness of the compression spring increases.

6. Conclusions

The paper presents calculations regarding the influence of the pressure spring stiffness on the opening and closing times of the low-pressure gas-phase injector. Based on the analyzes, the following conclusions were drawn.

1. The proposed model description of the operation of the gas injector showed the correlation of the results with the manufacturer's data. There was an reduction in the time to fully open by 2.77 % and increase in the time to fully close by 0.50 %. The model was found to be representative for comparison purposes.

2. Analyzing the times to full opening in the range of the compression spring stiffness (100… 2000) N/m, it was found that the time to full opening extended by 18.85% with a stiffness of 2000 N/m in relation to the stiffness of 100 N/m.

3. For the times to full closing in the stiffness range under consideration, it is reduced by 80.17% at 100 N/m compared to 2000 N/m.

4. The time-cross section determined at a stiffness of 2000 N/m is only 35.21% of the time-cross section at 100 N/m. From approx. 500 N/m, the time-cross sections decrease linearly with a slight decrease as the stiffness of the compression spring increases.

Acknowledgment

This research was financed through subsidy of the Ministry of Science and Higher Education of Poland for the discipline of mechanical engineering at the Faculty of Mechanical Engineering Bialystok University of Technology WZ/WM-IIM/4/2020.

References

1. **Ball, D.; Meng, X.; Weiwei, G.** 2020. Vehicle emission solutions for China 6b and Euro 7, Proceedings of the SAE Technical Papers 2020-01–06. https://doi.org/10.4271/2020-01-0654.
2. **Clairotte, M.; Suarez-Bertoa, R.; Zardini, A. A.; Giechaskiel, B.; Pavlovic, J.; Valverde, V.; Ciuffo, B.; Astorga, C.** 2020. Exhaust emission factors of greenhouse gases (GHGs) from European road vehicles, Environmental Sciences Europe 32: 125. http://dx.doi.org/10.1186/s12302-020-00407-5.
3. **Raslavičius, L.; Keršys, A.; Mockus, S.; Keršiene, N.; Starevičius, M.** 2014. Liquefied petroleum gas (LPG) as a medium-term option in the transition to sustainable fuels and transport, Renewable and Sustainable Energy Reviews 32: 513–525. http://dx.doi.org/10.1016/j.rser.2014.01.052.
4. **Wendeker, M.; Jakliński, P.; Czarnigowski, J.; Boulet, P.; Breaban, F.** 2007. Operational parameters of LPG fueled si engine - Comparison of simultaneous and sequential port injection, SAE Technical Papers 2007-01–2051. http://dx.doi.org/10.4271/2007-01-2051.
5. **Borawski, A.** 2015. Modification of a fourth generation LPG installation improving the power supply to a spark ignition engine, Eksploatacja i Niezawodnosc - Maintenance and Reliability 17: 1–6. http://dx.doi.org/10.17531/ein.2015.1.1.
6. **Mitukiewicz, G.; Dychto, R.; Leyko, J.** 2015. Relationship between LPG fuel and gasoline injection duration for gasoline direct injection engines, Fuel 153: 526–534. http://dx.doi.org/10.1016/j.fuel.2015.03.033.
7. **Warguła, Ł.; Kukla, M.; Lijewski, P.; Dobrzyński, M.; Markiewicz, F.** 2020. Influence of the use of Liquefied Petroleum Gas (LPG) systems in woodchippers powered by small engines on exhaust emissions and operating costs, Energies 13: 5773. http://dx.doi.org/10.3390/en13215773.
8. **Szpica, D.; Kusznier, M.** 2020. Modelling of the low-pressure gas injector operation, Acta Mechanica et Automatica 14: 29–35. http://dx.doi.org/10.2478/ama-2020-0005.
9. **Duk, M.; Czarnigowski, J.** 2012. The method for indirect identification gas injector opening delay time. Przeglad Elektrotechniczny 88(10B): 59–63.
10. **Mieczkowski, G.** 2017. Stress fields and fracture prediction for an adhesively bonded bimaterial structure with a sharp notch located on the interface, Mechanics of Composite Materials 53: 305–320. http://dx.doi.org/10.1007/s11029-017-9663-y.
11. **Marczuk, A.; Caban, J.; Aleshkin, A.V.; Savinykh, P.**

A.; Isupov, A. Y.; Ivanov, I. I. 2019. Modeling and simulation of particle motion in the operation area of a centrifugal rotary chopper machine, Sustainability (Switzerland) 11: 1–15. http://dx.doi.org/10.3390/su11184873.
12. **Bensetti, M.; Le Bihan, Y.; Marchand, C.** 2006. Development of an hybrid 3D FEM for the modeling of micro-coil sensors and actuators, Sensors and Actuators, A: Physical 129: 207–211. http://dx.doi.org/10.1016/j.sna.2005.11.060.
13. **Hung, N.B.; Lim, O.; Yoon, S.** 2017. Effects of structural parameters on operating characteristics of a solenoid injector, In Proceedings of the Energy Procedia 105: 1771–1775.
14. **Taghizadeh, M.; Ghaffari, A.; Najafi, F.** 2009. Modeling and identification of a solenoid valve for PWM control applications, Comptes Rendus - Mecanique 337: 131–140. http://dx.doi.org/10.1016/j.crme.2009.03.009.
15. **Passarini, L.C.; Pinotti, M.** 2003. A new model for fast-acting electromagnetic fuel injector analysis and design, Journal of the Brazilian Society of Mechanical Sciences and Engineering 25: 95–106. http://dx.doi.org/10.1590/S1678-58782003000100014.
16. **Czarnigowski, J.** 2012. Teoretyczno-empiryczne studium modelowania impulsowego wtryskiwacza gazu, Wydawnictwo Politechniki Lubelskiej, Lublin, ISBN PL 978-83-63569-09-9.
17. **Marčič, S.; Marčič, M.; Praunseis, Z.** 2015. Mathematical model for the injector of a common rail fuel-injection system, Engineering 7: 307–321. http://dx.doi.org/10.4236/eng.2015.76027.
18. **Szpica, D.; Mieczkowski, G.; Borawski, A.; Leisis, V.; Diliunas, S.; Pilkaite, T.** 2021. The computational fluid dynamics (CFD) analysis of the pressure sensor used in pulse-operated low-pressure gas-phase solenoid valve measurements, Sensors 21(24): 8287. http://dx.doi.org/10.3390/s21248287.
19. **Mieczkowski, G.; Szpica, D.; Borawski, A.; Diliunas, S.; Pilkaite, T.; Leisis, V.** 2021. Application of smart materials in the actuation system of a gas injector. Materials 14(22): 6984. http://dx.doi.org/10.3390/ma14226984.
20. **Vosken,** Valtek injector rail STD 3 ohm type 30 (4 cyl.) Available online: https://vosken.de/Valtek-injector-rail-STD-3-ohm-type-30-4-cyl (accessed on Apr 15, 2022).
21. **Passarini, L. C.; Nakajima, P. R.** 2003. Development of a high-speed solenoid valve: an investigation of the importance of the armature mass on the dynamic response, Journal of the Brazilian Society of Mechanical Sciences and Engineering 25: 329–335. http://dx.doi.org/10.1590/S1678-58782003000400003.
22. **Szpica, D.; Kusznier, M.** 2021. Model evaluation of the influence of the plunger stroke on functional parameters of the low-pressure pulse gas solenoid injector, Sensors (Switzerland) 21: 234. http://dx.doi.org/10.3390/s21010234.
23. **Yang, W. Y.; Cao, W.; Chung, T. S.; Morris, J.** 2020. Applied numerical methods using MATLAB®; Willey & Sons, ISBN 9780471698333.
24. **Shamdani, A. H.; Shameki, A. H.; Basharhagh, M. Z.; Aghanajafi, S.** 2006. Modeling and simulation of a diesel engine common rail injector in Matlab/Simulink, In Proceedings of the 14 th Annual (International) Mechanical Engineering Conference – May 2006 Isfahan University of Technology, Isfahan, Iran: 7p.
25. **Krichel, S. V; Sawodny, O.** 2011. Dynamic modeling of pneumatic transmission lines in Matlab/Simulink, In Proceedings of the International Conference on Fluid Power and Mechatronics - 17-20 August 2011, Beijing, China: 24-29. http://10.1109/FPM.2011.6045723.

D. Szpica, M. Kusznier

COMPUTATIONAL EVALUATION OF THE EFFECT OF PLUNGER SPRING STIFFNESS ON OPENING AND CLOSING TIMES OF THE LOW-PRESSURE GAS-PHASE INJECTOR

S u m m a r y

In the paper, an attempt was made to computationally demonstrate the effect of the plunger pressure stiffness on the opening and closing times of the low-pressure gas-phase injector as a filling of the research gap in this subject. Based on the presented mathematical model describing the operation of the injector, firstly the results were related to the manufacturer's technical data showing a shorter time to full opening by 2.77% and a longer time to full closing by 0.50%. On this basis, it was considered that the proposed model can be used for comparison purposes. In the assumed range of compression spring stiffness (100... 2000) N/m, it was shown that as the stiffness increases, the time to fully open decreases by 18.85%, while the time to fully closed decreases by 80.17%. Additionally, it is shown that the time-cross section as the stiffness of the compression spring increases can decrease up to 35.21% from the initial value. The obtained results can be useful in modeling the operation of an internal combustion engine or in the operational assessment of the gas injector condition.

Keywords: mechanical engineering, combustion engines, alternative fuel supply, LPG, modeling.

Received March 20, 2022
Accepted June 14, 2022